Int J Adv Manuf Technol (2013) 66:1343–1351
DOI 10.1007/s00170-012-4412-9

ORIGINAL ARTICLE

On the improvement of material formability in SPIF operation through tool stirring action

G. Buffa · D. Campanella · L. Fratini

Received: 5 December 2011 / Accepted: 23 July 2012 / Published online: 4 August 2012
© Springer-Verlag London Limited 2012

Abstract Single-point incremental forming (SPIF) is a quite new sheet-forming process which offers the possibility to deform complex parts without dedicated dies using a single-point tool and a standard three-axis CNC machine. The process mechanics enables higher strains with respect to traditional sheet-forming processes, but particular attention must be given to the maximum forming angle. In this paper, a new approach is proposed to enhance the material formability through a localized sheet heating as a consequence of the friction work caused by elevated tool rotational speeds. AA1050-O, AA1050-H24, and AA6082-T6 were utilized, and the reached temperatures were recorded by thermocouples, fixed to the sheet using a metal structure. A significant increase in the material formability was observed for both materials, and new formability curves have been built at the varying of the utilized rotational speed.

Keywords Incremental forming · Aluminum alloys · DRX · Microstructure

1 Introduction

In the recent years, world organizations and governments are pushing for a strong decreasing of conventional energy consumption and environmental pollution. In this way, the development of lightweight constructions is becoming a key factor, and advanced production technologies have to be developed to be competitive for this evolution. The use of the so-called lightweight alloys is continuously growing, and above these, aluminum alloys play a fundamental role being the most commonly utilized for applications in different fields, e.g., transportation, and chemical and food industries [1].

Among the innovative technologies of stamping proposed in order to answer to the requirement of a flexible and low-cost production, the incremental processes carry out a role of great importance. In these processes, the action of a tool, typically of small dimensions and simple geometry, moving along a prescribed trajectory, locally deforms in a progressive way the sheet metal, conferring the desired final shape. The idea that permeates all the incremental processes is to obtain three-dimensional geometries, starting from a sheet metal, thanks to the relative position progressively assumed by the tool (a simple hemispheric punch) and the sheet. In particular, the process taken into account in this research is the single-point incremental forming (SPIF): It represents the simplest and most economic incremental forming process, since it does not use fixed punch, as the deformation occurs only thanks to the effect of the tool that, completing a determined trajectory, locally deforms the sheet that is clamped along its border. Another fundamental characteristic of the considered process is that the clamping equipment is fixed, and the contact between the sheet and the tool occurs in the concave surface of the workpiece. The most relevant process parameters that govern the process are: the tool rotational speed, the tool feed rate, the so-called pitch, i.e., the sinking for each spire of the developed trajectory, the geometry, and material of the tool [2–4].

From the short description given above, it arises that the process is characterized by an elevated flexibility; as a

G. Buffa (✉) · D. Campanella · L. Fratini
Department of Chemical, Management, Computer Science and Mechanical Engineering, University of Palermo,
viale delle Scienze,
90128 Palermo, Italy
e-mail: gianluca.buffa@unipa.it

D. Campanella
e-mail: davide.campanella@unipa.it

L. Fratini
e-mail: livan.fratini@unipa.it

matter of fact, the same basic clamping fixture can be used to produce parts with different geometries, resulting in relevant cost savings with respect to traditional stamping operations, in which expensive dies must be dedicated to every single-part geometry. On the other hand, the process presents a few shortcomings with respect to traditional stamping operations that are the large times required to produce a part and the maximum drawing angle (that is always smaller than 90 degrees). Based on the above observations, it emerges that the process is particularly suited for niche production and prototypes.

One of the still open research front end is the enhancement of the material formability, especially for some alloys. In particular, magnesium alloys and 1xxx, 5xxx, and 6xxx series aluminum alloys with pre-hardening or heat treatment are characterized by poor formability at room temperature. In order to overcome such drawback and enhance the material formability, a few researchers have developed the SPIF process on pre-heated sheets. Zhang et al. [5] performed warm negative incremental forming experiments on AZ31 magnesium alloy sheets, 0.8 mm in thickness, focusing on the effect of different lubricating strategies suitable for high temperatures. They found both the use of $K_2Ti_4O_9$ whisker and the deposition of a porous ceramic coating on the magnesium sheets effective for the obtainment of proper lubrication conditions. Duflou et al. [6, 7] used a laser source in order to carry out a laser-assisted incremental forming process obtaining an improvement both in the materials formability and in the accuracy of the formed part. Ambrogio et al. [8] focused their attention on the formability limits of magnesium alloy AZ31 when warm incremental formed. They found a significant influence of temperature and tool depth step on the material formability, obtaining the maximum draw angle increase at a temperature of 250 °C; on the contrary a poor influence was observed for the tool diameter. Finally, as far as aluminum alloys are regarded, Salandro et al. [9] used pulsed electrical current, applied during the process, in order to increase the maximum forming angle of two 5xxx series aluminum alloys, namely AA5052 and AA5083. Three different temperature ranges were selected, and a formability enhancement, over traditional incremental forming processes, was found. In all the papers here cited, a warm forming process is obtained, and formability is significantly increased. Unfortunately, such approach results in increased costs partially losing one of the most important advantages of the process.

Further attempts were already made in order to use incremental forming with high-strength materials [10]. Working with titanium alloys, Fan et al. [11, 12] used electric heating in order to locally heat the blank reducing the material resistance and facilitating the tool-forming action. Recently, Taleb Araghi et al. [13] also followed the approach initially proposed by Duflou et al. carrying out laser-assisted single-point incremental forming operations.

In the paper, a new approach was developed in order to enhance the material formability through a local heating effect produced during the process by the tool rotation. It should be observed that, in literature, a few research works can be found focusing on the effect of the tool rotation on the process forces and final parts roughness. Durante et al. [14] found a decrease in the force trends at the increasing of the tool rotational speed in AA7075-O aluminum alloys; Hamilton and Jeswiet [15] analyzed the effects of high feed rates and rotational speeds on the sheet's exterior surface, thickness distribution, and grain size. However, in both the papers cited, no influence on the formability was observed because of the relatively low rotational speeds investigated. Other researches were recently aimed to investigate larger rotational speed ranges finding increased formability in 5xxx aluminum alloys [16].

In the present research, an experimental campaign was developed with the aim to produce conical frusta at the varying of the cone angle on AA1050 aluminum alloy in two different states, i.e., O and H24 and on AA6082-T6 aluminum alloy. The rotational speed varied in a wide range while fixed feed rate and vertical pitch have been selected. The locally reached temperature levels were measured by thermocouples placed on the reverse side of the blank with respect to the one formed by the tool. Finally, macro and micro observations were performed in order to explain the material microstructure modifications leading to the formability enhancement. For the utilized aluminum alloys, an increase in the maximum forming angle was actually obtained at the increase of the tool rotational speed.

2 The experimental setup

2.1 Fixture and machines

As the final aim of the present research was the enhancement of the material formability during SPIF operations, a main modification was introduced with respect to traditional incremental forming processes, i.e., the forming tool was put in rotation with extremely high speeds. In this way, although maintaining a lubricated contact in order to obtain a good finish of the formed surface, a local increase in the sheet temperature was produced by decaying of friction forces work into heat. As the temperature increase was localized near the forming tool, i.e., in the area of the material that is being formed in a given moment, no detrimental effect related to keeping the material at elevated temperatures for long times is produced. However, limited grain growth phenomena were produced while, in turn, a local softening

effect and increased formability of the material were observed. In Fig. 1, a sketch of the proposed process is shown.

The assigned tool path being a three-dimensional spiral, it included both the movement in the horizontal plane (i.e., the x–y table of the milling machine) and the penetration of the tool in the vertical direction (i.e., the movement along the z-axis). Therefore, the punch determined an almost pure stretching deformation mechanics on the fully clamped sheet. All the experiments were carried out on a Mazak vertical center nexus 410A-II three-axes NC milling machine. In order to develop the SPIF tests, a dedicated clamping fixture was utilized. A specimen sheet was put on a frame as shown in Fig. 1a and fixed by the blank holder with bolts. Figure 1b shows a sketch of the fixture at the end of the forming process.

2.2 Geometrical and technological parameters

Conical frusta were formed, at the varying of the draw angle, starting from 1-mm thick sheets of AA1050-O, AA1050-H24, and AA6082 aluminum alloys (Fig. 2).

All the developed geometries have a 150 mm major base diameter. The considered conical angle θ, shown in the

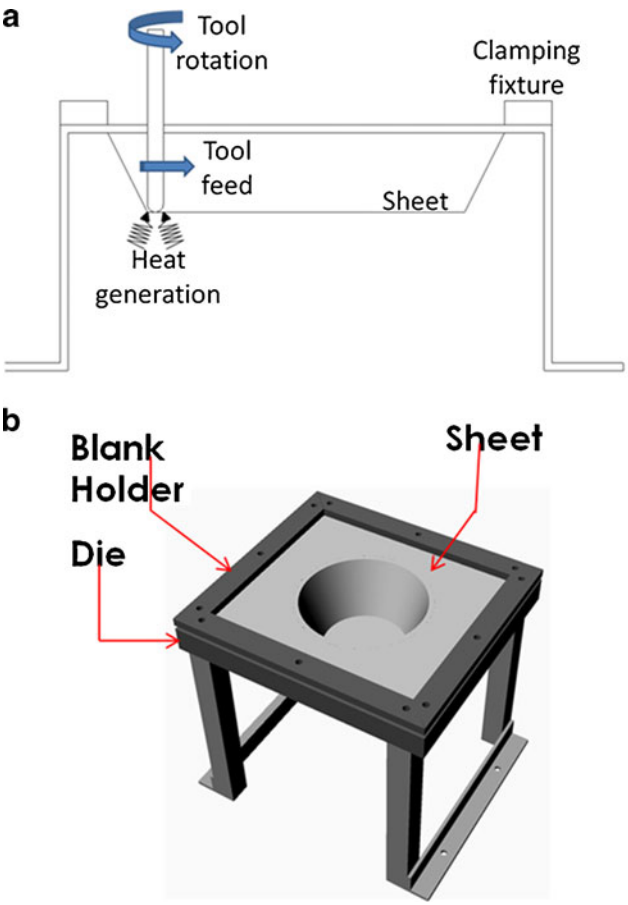

Fig. 1 **a** Sketch of the proposed process and **b** of the utilized clamping fixture

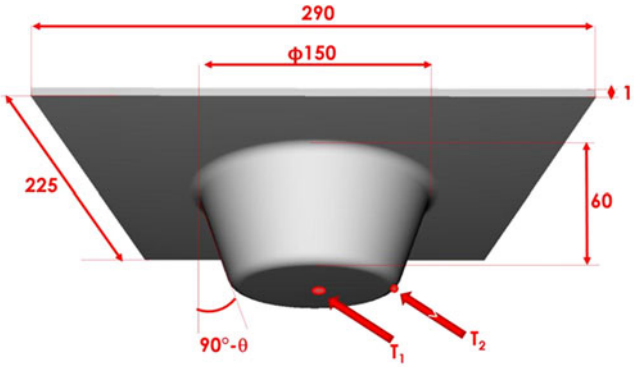

Fig. 2 Sketch of the formed part

Fig. 2, characterizes the obtained geometry. In this way, a larger angle corresponds to increased formability. An H13 steel cylindrical stylus with hemispherical head, 12 mm in diameter, was used as tool. A film of oil was applied to the blank to eliminate unwanted "milling" effects due to the elevated rotational speeds.

As far as the process technological parameters are regarded, fixed tool feed rate and vertical pitch were selected. The tool rotational speed ranged from 100 (room temperature tests, it will be indicated as "0 rpm" in the following case study) to 10,000 rpm. Table 1 summarizes the constant and variable parameters selected for AA1050, in two different states O and H24, and AA6082-T6. The time required to complete a geometry was about 28 min.

As previously indicated, the utilized blank materials were AA1050-O, AA1050-H24, and AA6082-T6 aluminum alloys; their flow rules of the materials at room temperatures were determined through preliminary tensile tests:

$$\mathrm{AA1050-O} \quad \sigma = 92\varepsilon^{0,14}[\mathrm{MPa}] \tag{1}$$

$$\mathrm{AA1050-H24} \quad \sigma = 112\varepsilon^{0,12}[\mathrm{MPa}] \tag{2}$$

$$\mathrm{AA6082-T6} \quad \sigma = 305\varepsilon^{0,21}[\mathrm{MPa}] \tag{3}$$

Table 1 Main process geometrical and technological parameters for the AA1050-O and AA1050-H24

Parameter	AA1050	AA6082
Tool diameter [mm]	12	12
Tool feed rate [mm/min]	2,000	2,000
Tool vertical pitch [mm]	1	1
Tool rotational speed [rpm]	100–10,000	100–10,000
Conical frustum major diameter [mm]	150	150
Draw angle θ	60°–80°	35°–60°

In order to understand the actual effect of the conferred heat flow on the mechanical properties of the sheets, flow stress curves were derived by both in-house experiments and literature data (Fig. 3). In particular, room temperature tests have been developed for the utilized batch of sheets and compared with the database found in Prased and Sasidhara [17]. Based on the good matching observed, we considered the literature data for temperatures higher than $T_{room.}$

2.3 Measurements and observations

Two thermocouples were placed on the surface of each sheet in order to measure the temperature values reached during the process. The first thermocouple was placed at the center of the sheets (T1, see again Fig. 2), and the second was automatically moved in order to measure the temperature on the fillet between the lateral and the bottom surfaces of the shaped cones (T2, see again Fig. 2). For more in details, the second thermocouple was mechanically fixed on the underside of the workpiece with respect to the side formed by the tool path, by means of a metal structure. Therefore, the structure was moved by a "step by step" motor, in order to assure that the thermocouple itself can be found, for each revolution of the tool, at the proper point, i.e., at the fillet between the lateral surface and the base of the cone, thus following the tool path and the blank deformation (Fig. 4).

As the tool followed a spiral path, it was possible to know its exact position at any given time. The structure attached to the bottom of the formed cone assured the proper z-position of the thermocouple while the motor, pulling the cursor using an inextensible wire, assured the proper radial position.

Finally, from the obtained parts, macro and micro observations of transverse sections were performed. For each test, specimens were cut, hot-mounted, polished, and then etched. Keller reagent was utilized for the two AA1050, while chromic acid was added to the previous solution to etch the AA6082-T6.

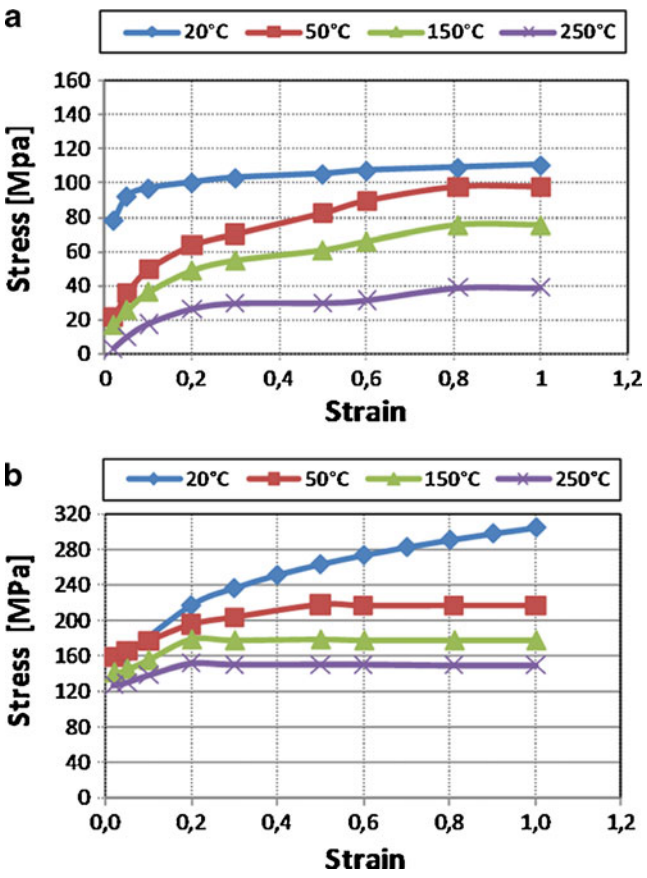

Fig. 3 Flow stress curves at the varying of temperature for **a** AA1050-H24 and **b** AA6082-T6

3 Obtained results

The first set of experiments was aimed toward finding the formability limit of the considered materials for the traditional SPIF process, i.e., with tool rotating speed equal to 100 rpm. For both AA1050-O and AA1050-H24, the maximum draw angle obtained was 65° while, for AA6082-T6, the maximum draw angle obtained was 40°. Hence, the draw angle was increased by steps of 2.5°, and for each angle value, a set of test trials were carried out at the increase of the tool rotational speed, till a defect-free part was obtained. In this way, different formability curves were obtained, as reported in Fig. 5a for AA1050-O and AA1050-H24 and in Fig. 5b for AA6082-T6. Each test was repeated three times, and an excellent repeatability was obtained as the three tests always gave the same response in terms of broken or sound part obtained. The tests corresponding to the limit curves shown in Fig. 5a and b have to be considered as safe.

Each curve delimits a formability area for a specific material: When a draw angle of 70° is selected, in order to have a sound part, a minimum tool rotational speed equal to 1,000 rpm must be used for the AA1050-O. In turn, when forming AA1050-H24 with the same angle, the minimum tool rotational speed increases to 4,000 rpm. Lower rotational speed will result in a broken part; higher speeds will result in a sound joint as well. As it can be seen from the figure, the maximum draw angle, equal to 75°, was obtained with the AA1050-O and tool rotating speed of 8,000 rpm. No further enhancement was observed with rotation speed equal to 10,000 rpm. In turn, a maximum formability angle of 72.5° was obtained for the AA1050-H24. As far as the AA6082-T6 is regarded, a maximum formability angle of 52.5°was observed corresponding to mandrel speed of 8,000 rpm.

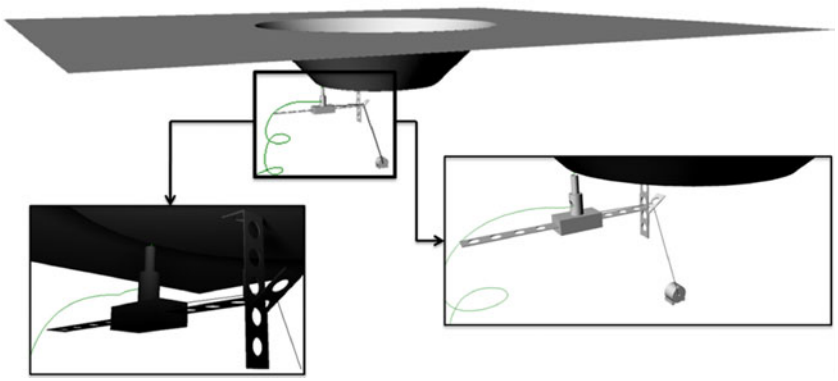

Fig. 4 Sketch of the measuring fixture utilized for the thermocouple T2

In order to understand the effect of the tool rotational speed on the material during the forming process, for each developed test, two thermocouples were fixed to the specimen as described in the previous paragraph (see again Fig. 2). In Fig. 6a, the temperatures measured during the test that characterized the maximum formability for the AA1050-H24 are reported while AA6082-T6 curves are reported in Fig. 6b.

The temperature values recorded by thermocouple T2 present, for each complete round of the tool on the assigned spiral path, a maximum peak corresponding to the moment in which the tool has just left the thermocouple and a minimum peak corresponding to the moment in which the tool is diametrically opposed to the thermocouple. For the sake of simplicity, in Fig. 5a and b, the envelopes of the maximum peaks are reported.

Looking at Fig. 6, it arises that both the thermocouples measure an increasing temperature during the process. This is due to the saturation of the thermal capacity of the sheet. However, a sort of steady state is observed in the sheets (thermocouple T1) indicating that a balance is reached between the thermal input and the thermal exchange with the environment. On the contrary, the temperature measured by the thermocouple T2 increases till the end of the process, as

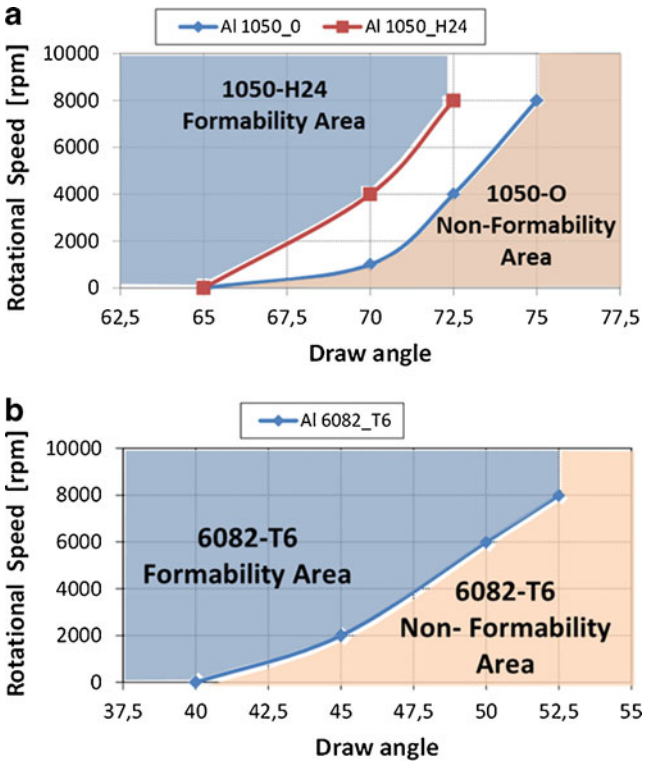

Fig. 5 **a** AA1050-O and AA1050-H24 and **b** AA6082-T6 formability limit curves

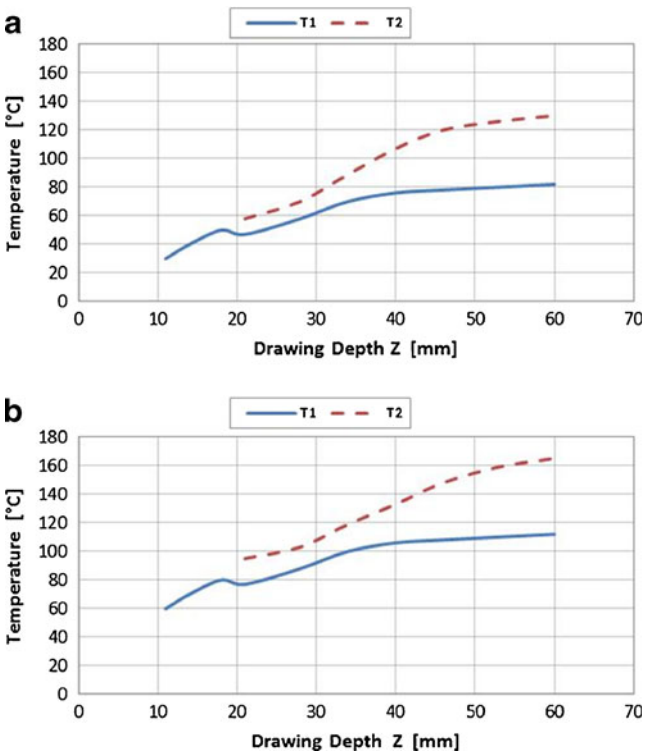

Fig. 6 Temperatures measued by the two thermocouples: **a** AA1050-H24, R=8,000 rpm, θ=72.5°, and **b** AA6082-T6, R=8,000 rpm, θ=52.5°

heat locally conferred by the friction forces work is larger than the one lost by the material emissivity and the convection with the surrounding air. As expected, maximum temperatures measured by thermocouple T2 are higher than temperature measured by T1, T2 being positioned right in correspondence with the heat source, i.e., the forming tool. A temperature value of about 130 °C is observed along the process for AA1050-H24 while about 160 °C is observed for AA6082-T6. It should be observed that, according to the material flow stress curves reported in Fig. 3, these temperature increases are sufficient to significantly decrease the mechanical properties of the material, producing a softening effect and resulting in enhanced formability. Finally, at the beginning of the process, at a drawing depth of about 20 mm, a local temperature decrease is observed for all the tested materials. This is due to a material thinning that can lead to failure, as will be explained more in detail in the following.

In order to compare the effects of different rotational speeds, the temperatures reached at the center of the sheet (Thermocouple T1) are shown in Fig. 7a for AA1050-H24 and Fig. 7b for AA6082-T6. The curves correspondent to the slowest velocity, i.e., 4,000 rpm for the AA1050-H24 and 2,000 rpm for the AA6082-T6, represent the lower formability limit, hence they are the first complete curves available for a given process condition (draw angle). As it can be seen from Fig. 5, with slower rotational speed, a complete part cannot be formed, and failure is observed after a few millimeters of drawing depth Z. On the other hand, for the two case studies presented in Fig. 7, the 10,000 rpm test was not performed, as complete forming was already obtained with lower rotational speed and confirmed with further tests performed with larger rotational speed values (e.g., 4,000, 6,000, and 8,000 rpm for the case study reported in Fig. 7b).

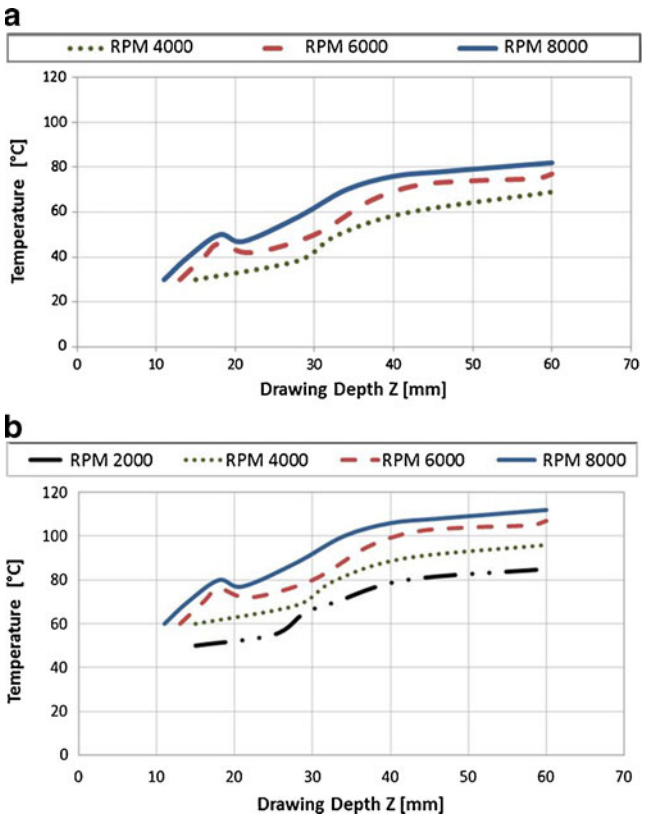

Fig. 7 Temperatures measured by the thermocouple T1 at the varying of the rotational speed: **a** AA1050-H24, θ=70° and **b** AA6082-T6, θ=45°

An average increase of about 10 °C is observed for an increase of 2,000 rpm in the tool rotational speed for all three alloys. Increasing the rotational speed from 4,000 to 8,000 rpm allowed obtaining a steeper angle with both the 1050-H24 and the 1050-O, increasing from 70° to 72.5° and from 72.5° to 75°, respectively. The same increase in the rotational speed produced an increase in the draw angle of 7.5°, corresponding to a maximum angle value of 52.5° for the AA6082-T6. As anticipated, both Fig. 7a and b show a local temperature decrease corresponding to a drawing depth of about 18 mm. These peaks are due to the necking of the material. In SPIF processes, the thickness of the inclined walls is reduced, following, for most of the part depth, the well-known sine law [1]; however, variations may occur. This phenomenon has already been observed by other researchers, especially for materials characterized by poor mechanical properties [15, 18]. In particular, Ambrogio et al. [18] indicated this as a critical point of the process: By measuring the forming force, a local decrease, analogous to the temperature decrease observed in the present work (see again Figs. 6 and 7), was observed and used to predict a failure. The local thinning, causing a reduction of the counterforce exerted by the sheet, results in a decrease of the friction forces work and, consequently, of the heat conferred to the sheet. If the selected draw angle is larger than the maximum forming angle for a given tool rotational speed, the temperature will continue its decreasing till a crack will be observed in the formed part. The macro image of the transverse section of an AA1050-H24 formed part is presented together with the thickness profile along the drawing depth z (Fig. 8a and b). A similar trend was obtained for the AA6082-T6 specimens, confirming the analogous temperature loss observed in Fig. 6b.

In order to investigate the effects of the high rotational speed conferred to the tool from a microstructural point of view, transverse sections were cut from the lateral surfaces of each formed part. In Fig. 9, micro images from different AA6082-T6 formed parts are shown.

All the figures refer to tests obtained with a drawing angle of 45°. As it can be observed, no significant variation, with respect of the parent material, is found in the joint

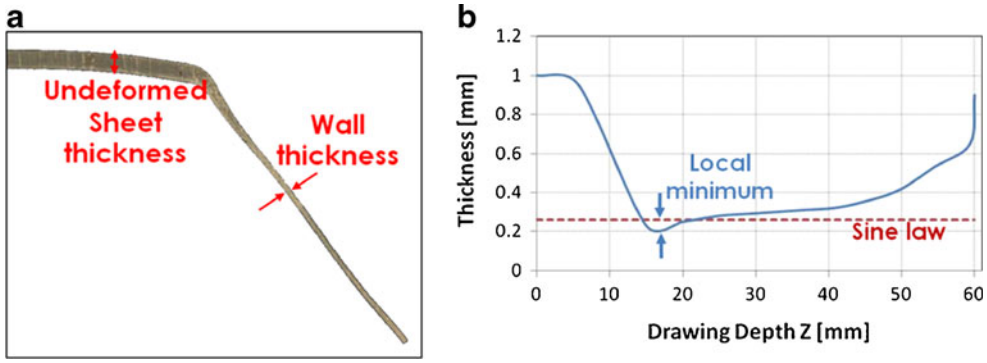

Fig. 8 **a** Macro image of a transverse section of the joint and **b** thickness along the drawing depth (AA1050-H24, θ=75°)

microstructure as the tool rotation speed increases up to 4,000 rpm (Fig. 9a and b). When a rotation of 10,000 rpm is selected, a finer and more equiaxed grain is observed close to the bottom of the formed part, i.e., near the last contact position between the tool and sheet before the end of the process (Fig. 9c). On the other hand, if a specimen is cut form the lateral surface of the cone at about half depth ($z\cong$ 30 mm), a more elongated and grown grain is observed. In other words, when the tool comes in contact with the sheet during the process, dynamic recrystallization (DRX) phenomena occurs, generating a smaller and equiaxed grain. As the tool continues its motion along the assigned path, the recrystallized area is subjected to further stirring, resulting in an elongation of the grain and, due to the concurrent effect of the temperature, in grain growth phenomena. This last aspect is more visible on specimens cut from half depth (Fig. 9d) of the cones because these areas are subjected to deformation and temperature effects for a longer time. Conversely, almost no elongation is found on specimens cut from the lateral surface near the bottom of the part, as the material of those areas did not experience any additional stirring after the DRX took place, and temperature decreased rapidly due to the end of the process.

Figure 10 shows the average grain dimension measured on specimens obtained with a draw angle of 45°, at the varying of the tool rotation, in analogous locations of that described for Fig. 9c.

From each micro image, several grains were measured, and in Fig. 10, the average values of the equivalent grain diameter are reported. It is observed that the grain dimension is about constant and equal to the one of the parent material, i.e., about 65 μm, for rotational speeds values smaller than 6,000 rpm. From this speed on, the measured average size dramatically decreases to a value of about 20 μm, indicating that the activation energy needed for the DRX process has been reached. Grain growth phenomena occur, as explained with regard to Fig. 9, and that is why the observed average size is not in the range of 6–12 μm as it could be expected after a

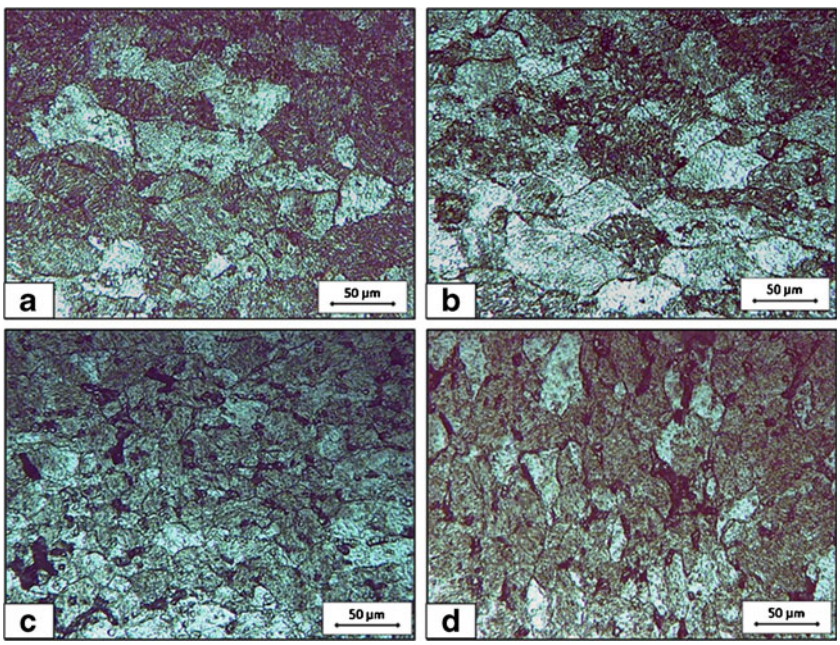

Fig. 9 ×250 magnification of the microstructure of AA6082 (θ=45°): **a** parent material, **b** 4,000, **c** 10,000, and **d** 10,000 rpm, half depth

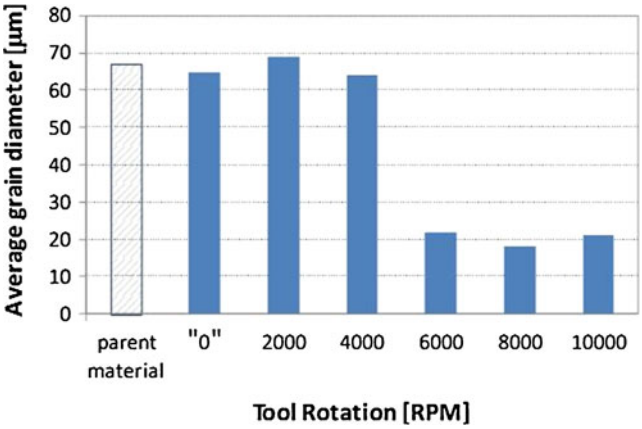

Fig. 10 Average grain dimension in AA6082 (θ=45°) formed parts

DRX process of AA6082-T6 aluminum alloys [19]. It is worthy to notice that, besides the microstructural modifications described above, the local heating also produces effects on the surface quality of the parts. In particular, a slight "orange peel" surface is observed as temperature increases, i.e., as rotational speed increases. However, in this paper, no quantitative roughness measurement has been carried out being the main focus the formability enhancement analysis.

Finally, microhardness tests were performed along the drawing depth of the formed parts as shown in Fig. 11 for the AA6082-T6. Similar trends were obtained for the two AA150 alloys.

As no significant variation was observed in a single specimen at the varying of the drawing depth, just the average value was reported for each case study. For the sake of simplicity, consistent with what is shown in the previous Fig. 10, just the AA6082-T6 results are reported. A slight increase, with respect to the parent material hardness, is observed for the "0 rpm" case study, i.e., the one corresponding to "traditional" incremental forming (please note that the actual tool rotation used for this set of tests is 100 rpm, as highlighted in Table 1). This phenomenon, due to the effect of the work hardening, was already observed by other authors for different materials [16, 20]. As the rotational speed increases, temperature increases, and slightly smaller hardness values are found. When rotational speed is equal or higher than 6,000 rpm, the microhardness falls down due to the prevalent effect of the temperature. It should be noticed that the observed values are larger than what they would be if DRX did not occur. In fact, due to the effect of temperature, the precipitates density decreases, as part of the precipitates go in solution with the matrix material. In this way, an opposite effect to the precipitation hardening phenomenon is obtained, and, of course, a local material softening occurs. However, the reduction of the average grain dimension, which is obtained with rotational speeds in excess of 6,000 rpm, contrasts the material softening due to the reduction of the precipitates, resulting in slightly larger hardness values [21].

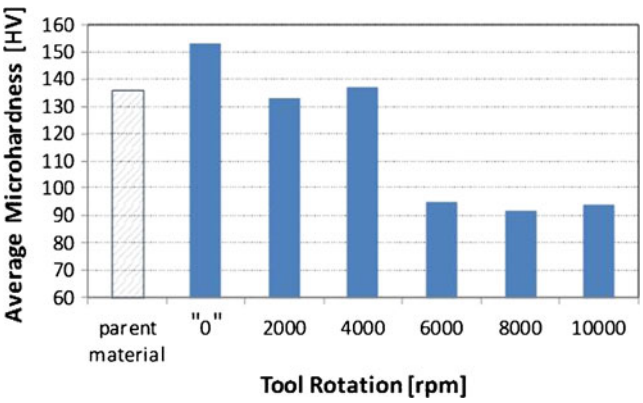

Fig. 11 Microhardness values in AA6082 (θ=45°) formed parts

4 Conclusions

In the paper, the results of an experimental campaign on a new approach for formability enhancement in single-point incremental forming process are presented. Extremely high tool rotational speeds have been used to produce a local increase in the temperatures of AA1050-O, AA1050-H24, and AA6082-T6 aluminum alloys, selected for their poor formability at room temperature.

For all the utilized aluminum alloys, a significant enhancement in the sheet formability was obtained, regardless of the initial sheet conditions, namely, fully annealed, strain-hardened, or heat-treated. Maximum draw angle increase of 7.5°, 10°, and 12.5°, with respect to the traditional SPIF process, was found for AA1050-H24, AA1050-O, and AA6082-T6, respectively. The causes of this improvement were analyzed by the use of thermocouples, the observation of the transverse section profiles, and grain and microhardness measurements.

It is found that the largest draw angles can be reached because a dynamic recrystallization takes place, due to the concurrent effect of temperature, strain, and strain rate. However, grain growth phenomena occur during the process, especially in the sheet areas that are deformed first, resulting in a final grain dimension of about 20 µm with a slightly elongated shape.

The proposed approach is very promising in order to obtain a low-cost formability improvement, as no additional external heat sources are needed.

In the future, a detailed study on the lubrication will be performed with the aim of analyzing its influence on the sheet roughness and on the temperatures reached, optimizing the maximum draw angle obtainable with a given tool rotational speed.

Acknowledgments This work was made using MIUR (Italian Ministry for University and Scientific Research) funds.

References

1. Kleiner M, Geiger M, Klaus A (2003) Manufacturing of lightweight components by metal forming. CIRP Ann 52:521–542
2. Jeswiet J, Micari F, Hirt G, Bramley A, Duflou J, Allwood J (2005) Asymmetric single point incremental forming of sheet metal. CIRP Ann 54(2):88–114
3. Iseki H, Naganawa T (2002) Vertical wall surface forming of rectangular shell using multistage incremental forming with spherical and cylindrical rollers. J Mater Process Technol 130:657–662
4. Hagan E, Jeswiet J (2004) Analysis of surface roughness for parts formed by CNC incremental forming. IMECHE part B J of Eng Manuf 218B10:1307–1312
5. Zhang Q, Xiaoa F, Guoa H, Li C, Gaob L, Guoc X, Hand W, Bondareve AB (2010) Warm negative incremental forming of magnesium alloy AZ31 sheet: new lubricating method. J Mater Process Technol 210:323–329
6. Duflou JR, Callebaut B, Verbert J, De Baerdemaeker H (2007) Laser assisted incremental forming: formability and accuracy improvement. CIRP Ann 56(1):273–276
7. Duflou JR, Callebaut B, Verbert J, De Baerdemaeker H (2008) Improved SPIF performance through dynamic local heating. Int J of Mach Tools and Manuf 48(5):543–549
8. Ambrogio G, Filice L, Manco GL (2008) Warm incremental forming of magnesium alloy AZ31. CIRP Ann 57(1):257–260
9. Salandro WA, Jones JJ, McNeal TA, Roth JT (2010) Formability of Al 5xxx sheet metals using pulsed current for various heat treatments. J Manuf Sci Eng Trans ASME 132(5):1-11
10. Hino R, Yoshida F, Nagaishi N, Naka T (2008) Incremental sheet forming with local heating for lightweight hard-to-form material. Int J of Mod Phys B 22(31–32):6082–6087
11. Fan G, Sun F, Meng X, Gao L, Tong G (2010) Electric hot incremental forming of Ti-6Al-4V titanium sheet. Int J Adv Manuf Technol 49(9–12):941–947
12. Fan G, Gao L, Liu P, Wu Z, Meng X, Tong G (2010) Technology analysis and optimization for electric hot incremental forming of Ti-6Al-4V sheet. J of Nanjing Univ of Aeronaut and Astronaut 42 (2):238–243
13. Taleb Araghi B, Göttmann A, Bergweiler G et al (2011) Investigation on incremental sheet forming combined with laser heating and stretch forming for the production of lightweight structures. Key Eng Mater 473:919–928
14. Durante M, Formisano A, Langella A, Memola Capece Minutolo F (2009) The influence of tool rotation on an incremental forming process. J Mater Process Technol 209:4621–4626
15. Hamilton K, Jeswiet J (2010) Single poin incremental forming at high feed rates and rotational speeds: surface and structural consequences. CIRP Ann 59(1):311–314
16. Otsu M, Matsuo H, Matsuda M, Takashima K (2010) Friction stir incremental forming of aluminum alloy sheets. Steel Res Int 81 (9):942–945
17. Prased YVRK, Sasidhara S (1997) Hot working guide—a compendium processing maps. ASM Int., Materials Park, OH
18. Ambrogio G, Filice L, Micari F (2006) A force measuring based strategy for failure prevention in incremental forming. J Mater Process Technol 177:413–416
19. Fratini L, Buffa G (2005) CDRX modelling in friction stir welding of aluminum alloys. Int J of mach Tools and Manuf 45(10):1188–1194
20. Rattanachan K, Chungchoo C (2009) Formability in single point incremental forming of dome geometry. AIJSTPME 2(4):57–63
21. Barcellona A, Buffa G, Contorno D, Fratini L, Palmeri D (2005) Microstructural changes determining joint strength in friction stir welding of aluminium alloys. Adv Mater Research 6–8:591–598